Electron Beam Synthesis and Characterization of Poly(vinyl alcohol)/Montmorillonite Nanocomposites

Safaa G. Abd Alla,[1] Horia M. Nizam El-Din,[2] Abdel Wahab M. El-Naggar[1]

[1]*Department of Radiation Chemistry, National Center for Radiation Research and Technology, Nasr City, Cairo, Egypt*
[2]*Department of Polymer Chemistry, National Center for Radiation Research and Technology, Nasr City, Cairo, Egypt*

Received 29 August 2005; accepted 18 January 2006
DOI 10.1002/app.24370
Published online in Wiley InterScience (www.interscience.wiley.com).

ABSTRACT: Poly(vinyl alcohol) (PVA)/montmorillonite clay (MMT) nanocomposites in the form of films were prepared under the effect of electron beam irradiation. The PVA/MMT nanocomposites gels were characterized by X-ray diffraction (XRD), differential scanning calorimetry (DSC), thermogravimetric analysis (TGA), scanning electron microscopy (SEM), and mechanical measurements. The study showed that the appropriate dose of electron beam irradiation to achieve homogeneous nanocomposites films and highest gel formation was 20 kGy. The introduction of MMT (up to 4 wt %) results in improvement in tensile strength, elongation at break, and thermal stability of the PVA matrix. In addition, the intercalation of PVA with the MMT clay leads to an impressive improved water resistance, indicating that the clay is well dispersed within the polymer matrix. Meanwhile, it was proved that the intercalation has no effect on the metal uptake capability of PVA as determined by a method based on the color measurements. XRD patterns and SEM micrographs suggest the coexistence of exfoliated intercalated MMT layers over the studied MMT contents. The DSC thermograms showed clearly that the intercalation of PVA polymer with these levels of MMT has no influence on the melting transitions; however, the glass transition temperature (T_g) for PVA was completely disappeared, even at low levels of MMT clay. © 2006 Wiley Periodicals, Inc. J Appl Polym Sci 102: 1129–1138, 2006

Key words: nanocomposites; electron beam irradiation; poly(vinyl alcohol) (PVA); montmorillonite clay

INTRODUCTION

Polymer/clay nanocomposites have been reported to exhibit unique properties and lead to environmentally friendly and inexpensive plastic composites. Improved flame retardancy, increased thermal stability, improved mechanical properties, and decrease in permeability are some of the properties that can be obtained.[1–3] The dispersion of the clay within the polymer has significant influence on the properties of the material because of the hydrophilicity of clays, which hinders the formation of homogeneous dispersion in organic polymers.[4,5] When clay is not well dispersed, either an intercalated or a delaminated nanocomposite is formed.[6] Intercalated nanocomposites consists of well-ordered layers in which registry is maintained between the clay layers, while this registry is lost in delaminated, also known as exfoliated, nanocomposites. The formation of delaminated nanocomposites seems to lead to a greater enhancement of mechanical properties than is observed for intercalated systems. It has been suggested that layered materials may be beneficial to the enhancement of polymer properties.

The hybridization of organic material (polymer) with the inorganic particles with nano-scale (clay) was the topic of many research works in the past several years. The morphology and thermal stability of poly(methyl methacrylate)/clay nanocomposites, prepared by emulsion polymerization using a cationic initiator in the presence of free surfactant, was investigated.[7] In addition, the thermal degradation and flame retardant mechanism of polystyrene–clay nanocomposites prepared chemically by the bulk technique was reported.[8] Polyamide–clay nanocomposites preparation by melt compounding has also attracted many authors: processing degradation[9] and thermal degradation behavior.[10]

Sodium montmorillonite (MMT) is a naturally occurring 2:1 phyllosilicate, capable of forming suspension in water. Poly(vinyl alcohol) (PVA) is water soluble, nontoxic, highly hydrophilic with a wide industrial applications, and most importantly good film forming. The hydrophilic character of MMT clay allows dispersion of these inorganic crystalline layers in water-soluble polymers such as poly(ethylene oxide)[11] and poly(vinyl alcohol).[12,13] In the present work, PVA/MMT clay nanocomposites in the form of network structure were prepared under the effect of electron beam irradiation. The formed nanocomposites

Correspondence to: A. W. M. El-Naggar (ab_nagga@yahoo.com).

were characterized by X-ray diffraction (XRD), thermogravimetric analysis (TGA), differential scanning calorimetry (DSC), scanning electron microscopy (SEM), and mechanical testing. In addition, the capability of PVA/MMT nanocomposites to absorb copper ions was investigated.

EXPERIMENTAL

Materials

Sodium montmorillonite clay (MMT) used in this study has a cation-exchange capacity of 74.6 mequiv./100 g and was collected from the Nile river banks. However, before use, the MMT clay was purified by repeated washing cycles and filtration to remove strange matters. The MMT suspension in distilled water at room temperature was then sonicated for 30 min, allowed to stand over night, filtered, and left to dry in vacuum oven. The poly(vinyl alcohol) homopolymer (PVA) used in this study was of laboratory grade; it is a fully hydrolyzed polymer in the form of powder, with average molecular weight of 106,000, T_g of 99°C, T_m of 258°C, solubility parameter of 13.4, and it was purchased from Laboratory Rasayan, Cairo, Egypt. The homopolymer was used without further purification.

Preparation of PVA/MMT clay nanocomposites

PVA/clay nanocomposites were prepared by a solution-intercalation film method. The PVA powder was dissolved in distilled water at 95°C; while room temperature-distilled water was used to form suspensions of the sodium montmorillonite clay. Different compositions of polymer solutions and MMT clay suspension with different clay contents (up to 5 wt %) were mixed with continuous stirring for 2 h, and sonicated for 30 min. The polymer/clay solutions were allowed to stand over night to remove air bubbles and were then poured into glass dishes to obtain films of appropriate thickness.

Electron beam irradiation

Irradiation was carried out on the electron accelerator facility (1.5 MeV and 25 kW) of the National Center for Radiation Research and Technology (Cairo, Egypt), in which the required doses were obtained by adjusting the electron beam parameters and conveyer speed.

Determination of gel fraction

Samples of the prepared nanocomposites films were accurately weighted (W_0) and then extracted with distilled water using soxhlet system for 6 h. After extraction, the samples were removed and dried in a vacuum oven at 50°C to a constant weight (W_1). The soluble fraction was calculated according to the following equation:

$$\text{Sol fraction (\%)} = [W_0 - (W_1)/W_0] \times 100$$

$$\text{Gel fraction (\%)} = 100 - \text{Sol fraction}$$

Water resistance measurements

A known dry weight of the insoluble PVA/MMT nanocomposites films (W_0) was immersed in distilled water for 24 h at room temperature. The samples were removed and blotted on a filter paper to remove the excess water on the surface and weighed (W_1). The percentage swelling was calculated according to the following equation:

$$\text{Water uptake (\%)} = [W_1 - W_0)/W_0] \times 100.$$

The water uptake (%) was taken as a measure for water resistance.

X-ray diffraction analysis

X-ray diffraction (XRD) experiment of the samples was performed at room temperature by a Philips PW 1390 diffractometer (30 kV,10 mA) with copper target irradiation at a scanning rate of 8°/min in a 2θ range of 4°–90°.

Color strength and measurements

A computerized micro-colorimeter unit made by Dr. Bruno Lange, GmbH, Konigsweg 10, D-1000, Berlin, Germany, was used for color measurements. The L^*, a^*, and b^* system used is based on the CIE-color Triangle (Commission International De E´ Clair Units X, Y, and Z). In this system, the L^* value represents the dark–white axis, a^* represents the green–red axis, and b^* represents the blue–yellow axis. The L^*, a^*, and b^* values of pure PVA film was first measured and taken as references. The color strength of the samples either before or after soaking in copper salt solution was calculated according to the following equation, in which each value is the average of five measurements along the sample:

$$\Delta E^* = \sqrt{(\Delta L^*)^2 + (\Delta a^*)^2 + (\Delta b^*)^2}$$

Differential scanning calorimetry

The differential scanning calorimetry (DSC) thermograms were carried out on Perkin–Elmer DSC-7. A heating rate of 10°C min^{-1} was utilized under flowing nitrogen at a rate of 20 mL min^{-1}. The recorded glass

transition temperature was taken as the temperature at which one half of the change in heat capacity had occurred.

Thermogravimetric analysis

The thermogravimetric analysis (TGA) studies were carried out on a Shimadzu-50 instrument (Japan) at a heating rate of 10°C min^{-1} under flowing nitrogen of 20 mL min^{-1} over a temperature range from room temperature up to 500°C. Duplicate runs of the TGA thermograms of some PVA/MMT systems were performed to check the reproducibility of the thermal data. The standard deviation for the percentage weight loss was calculated to be ±0.24%, while that for the $T_{1/2}$ and T_{max} was 2°C.

Scanning electron microscopy

The morphology of the fracture surfaces of the PVA and PVA/MMT nanocomposites was examined. The scanning electron micrographs were taken with a JSM-5400 instrument (Joel, Japan). A sputter coater was used to pre-coat conductive gold onto the fracture surfaces before observing the microstructure at 25 kV.

Tensile mechanical measurements

Mechanical parameters, including tensile strength and elongation at break point, were measured at room temperature using an Instron machine (model 1195, High Wycombe, UK) at a crosshead speed of 5 mm min^{-1}. PVA/MMT clay nanocomposites films were cut with a die into dumbbell shape of 40 mm length and 4 mm width. The recorded value for each mechanical parameter is the average of four measurements.

RESULTS AND DISCUSSION

Clay materials have open three-dimensional framework structures with channels and interconnecting cavities of SiO_4 and AlO_4 tetrahedral. Since aluminum is trivalent, the lattice carries a negative charge. This charge is balanced by alkali or alkaline earth cations, which do not occupy fixed position but are free to move in the channels of the lattice framework.[14] The montmorillonite clay has a 2:1 layered structure; Al^{3+} can isomorphously replace Si^{4+} in a number of silicate structures [two layers of SiO_4 tetrahedral and one AlO_4 tetrahedral].

A few weight percent of layered silicates that are properly dispersed throughout the polymer matrix would create much higher surface area for polymer/filler interaction as compared to conventional composites. There are two different types of polymer layered silicate nanocomposites (PLSNs) depending on the strength of interfacial interactions between the polymer matrix and layered silicate.[15] Intercalated nanocomposites result from the penetration of polymer molecules into the interlayer space, while exfoliated nanocomposites result when individual clay layers are separated in a continuous polymer matrix by average distances that depends on clay loading.

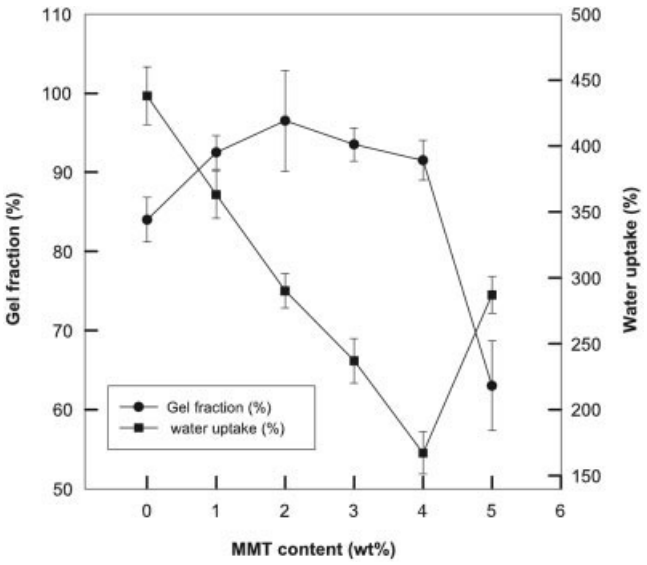

Figure 1 Gel fraction (%) and water uptake (%) as a function of MMT content for PVA/MMT nanocomposites gels formed at a dose of 20 kGy of electron beam irradiation.

Gel fraction and water resistance

Preliminary experiments showed that the percentage gel fraction of PVA at doses 10, 20, and 30 kGy, was 60, 86, and 90%, respectively. Since the objective of the present work is to form nanocomposites gels, the dose 20 kGy was used throughout this work. Figure 1 shows the percentage gel fraction and water uptake as a function of MMT content for PVA/MMT nanocomposites films formed at a constant dose 20 kGy of electron beam irradiation. It can be seen that the percentage gel fraction of pure PVA increase to reach a value of ~95% at MMT content of 2 wt %, and then decrease progressively with increasing MMT content to reach a value of ~67% at MMT content of 5 wt %. The distribution of MMT nanoparticles in the crystalline region of PVA would eventually facilitate the exposure of additional sites to electron beam irradiation leading to higher gel fractions than pure PVA. However, when PVA was loaded with higher levels of MMT, an opposite trend was observed, in which it seems that MMT nanoparticles block limited number of sites leading to a decrease in gel fraction.

An opposite trend can be observed in the relationship between the MMT content and water uptake of PVA/MMT nanocomposites. The introduction of MMT clay up to 4% leads to an obvious decrease in

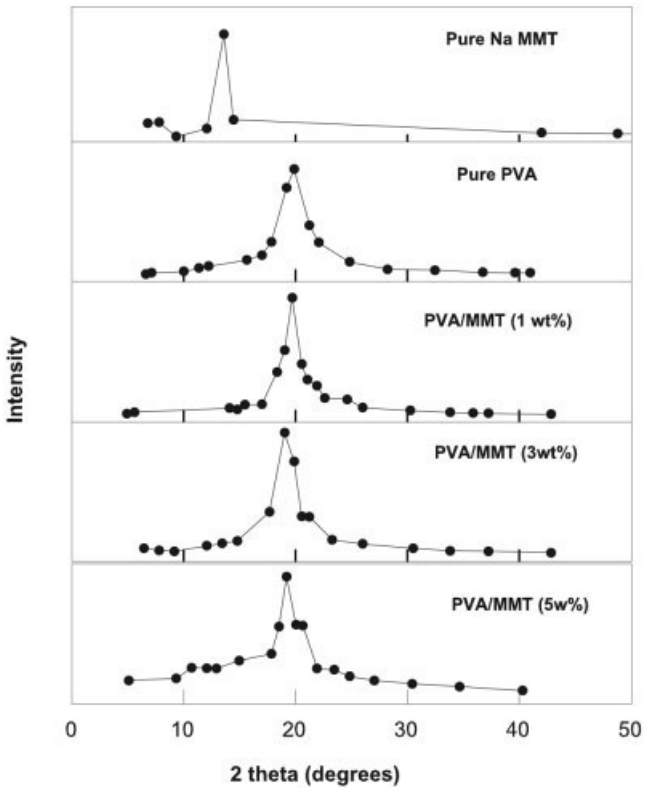

Figure 2 XRD patterns of pure MMT, pure MMT clay, and PVA/MMT nanocomposites.

water uptake (water resistance). This decrease in water uptake is due to the strong interaction between MMT and PVA matrix, which leads to the formation of bound polymer, which is close to the reinforcing filler leading to the restriction of the water absorption.

XRD analysis of PVA/MMT nanocomposites

Figure 2 shows the XRD patterns of pure PVA, pure MMT, and PVA/MMT nanocomposites with various MMT contents and Table I shows the results of the XRD analysis. XRD reports the spacing between ordered layers of the d_{001} or basal spacing, in which water expanded sodium clay normally exhibits a peak associated with a spacing of 12.5 Å.[16] The absence of this basal peak is commonly taken as evidence for a high dispersion of clay platelets, whereas a peak associated with higher spacing would indicate intercalated nanocomposites. As shown in Figure 2, the diffraction peak corresponding to MMT clay was disappeared completely in the XRD patterns of PVA/MMT nanocomposites, reflecting the dispersion and the intercalation of MMT. The intensity of this peak decreases as the amount of MMT increases as shown in Figure 2 and Table I in agreement with the findings of Strawhecker and Manias[13] and Yu et al.[17] The crystalline behavior is suppressed by the introduction of sodium clay into polymer matrix in the form of intercalated structure.

Metal absorption by PVA/MMT nanocomposites

Poly(vinyl alcohol) as a highly hydrophilic polymer was widely used to absorb heavy metals and dyestuffs from wastewater. However, the formation of MMT polymer/layered silicate hybrids results in a significant decrease in water uptake. In the present work, the capability of PVA/MMT nanocomposites to absorb Cu^{2+}, which is characterized with a distinct color, was investigated. In this experiment, the change and distribution of color as a function of immersion time in Cu^{2+} salt solutions containing a constant concentration was measured. A method based on color measurements was used, in which not only the color intensity was recorded but also the change in the color components forming the original color can be determined. In this regard, the 0 and 100 integers of the L^* value represent the standard darkness and whiteness, whereas the positive value of a^* and b^* represent the red and yellow and the negative value represent the green and blue components, respectively.

Figures 3 and 4 show the change in color intensity (ΔE^*) and the different color parameters (L^*, a^*, and b^*) as a function of immersion time in Cu^{2+} solutions at constant concentration for pure PVA and PVA/MMT nanocomposites films at constant weights. It should be noted that the zero point data on the X-axis represent the color parameters for the different films before immersion in Cu^{2+} solution. In general, there is a critical point, at which maximum color intensity was achieved, depending on the polymer composition. While pure PVA and PVA/MMT (3%) reach equilibrium (highest color intensity) after 1 h, the PVA/MMT (5%) reaches equilibrium after 3 h. Since the PVA/MMT films were not completely transparent due to the dispersion of MMT nanoparticles, the color intensity data at any time of immersion have to be subtracted from the corresponding data for pure PVA to determine the actual capability (Fig. 3). This procedure showed clearly that the introduction of MMT clay does not affect the capability of PVA to absorb Cu^{2+} ions.

TABLE I
Summary of XRD Patterns of Pure PVA, Pure MMT Clay, and PVA/MMT Nanocomposites with Various Contents

Polymer composition	2θ	D (Å)	Intensity
Pure MMT	13.60	6.51	0.400
Pure PVA	19.90	4.46	0.963
PVA/MMT (1 wt %)	19.72	4.50	0.710
PVA/MMT (3 wt %)	19.04	4.66	0.645
PVA/MMT (5 wt %)	19.21	4.62	0.318

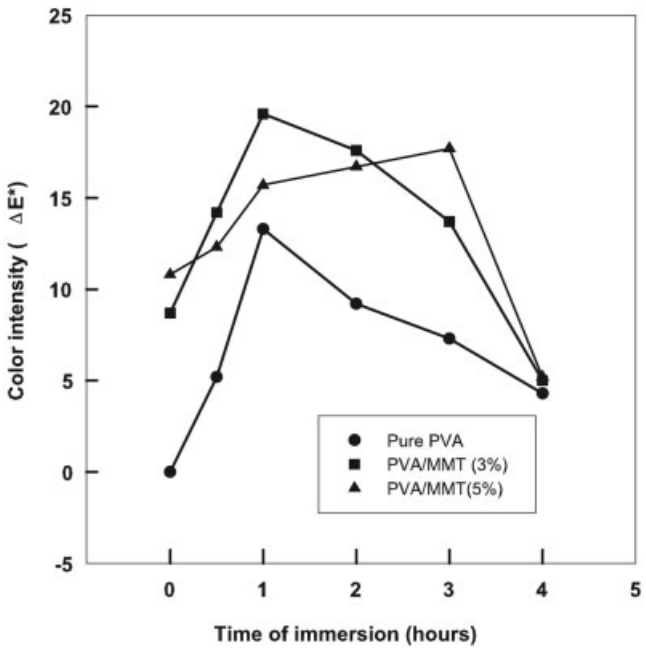

Figure 3 Color intensity of pure PVA polymer, PVA/MMT(3%), and PVA/MMT (5%) nanocomposites films formed at a dose of 20 kGy of electron beam irradiation, before and after immersion in copper salt solutions for various lengths of times.

As shown in Figure 4, it can be seen that the PVA/MMT films before or after immersion in Cu^{2+} solutions possess a darker shade than those of pure PVA in terms of the L^* values. In addition, the deepness in color increases slightly with increasing the time of immersion. The main effects can be seen in the values of a^* and b^* components, in which the films of pure PVA, before or after immersion in Cu^{2+} solutions displayed a color composed of green and yellow components. Similar trends can be observed in the case of PVA/MMT nanocomposites after immersion in Cu^{2+} solutions. It is interesting to find that PVA/MMT films, before immersion, possess colors composed of red and yellow components, and convert to green and yellow components after absorbing Cu^{2+}. Based on these results, it can be concluded that the presence of the MMT clay does not affect the characteristic color of Cu^{2+} ions and hence the capability of PVA polymer.

Glass and melting transitions of PVA/MMT nanocomposites gels

PVA polymer has a glass transition at ~70°C and a melting at ~225°C. DSC technique was used to investigate the effect of montmorillonite (MMT) content on the glass and melting transitions of PVA, before and after intercalation with different contents of MMT. Figure 5 shows the DSC thermograms of pure PVA and PVA/MMT nanocomposites gels at various levels of MMT. The upper figure shows the DSC traces for the glass transition temperature (T_g) of neat PVA polymer. A systematic study of the DSC traces for PVA/MMT nanocomposites with increased MMT content (1–5%) does not detect any glass transition between room temperature and 120°C. However, the DSC traces for these nanocomposites showed clearly the melting transition of the PVA polymer, in which there was nearly no effect of the MMT content. It seems that the glass transition temperature of the intercalated nanocomposites is weak or too broad to measure, or it was suppressed due to the polymer confinement in accordance with previous work.[13,18,19] This suggests that in these systems the inorganic layers affect all the polymer morphology, even though the maximum MMT content is still low with respect to the PVA matrix.

Thermal stability of PVA/MMT nanocomposites gels

Thermal stability may represent an important property in polymer/layered silicate nanocomposites (PLSNs). It is generally accepted that the improvement in thermal stability is related to barrier properties and the radical-trapping effect of clay platelets. Thermogravimetric analysis (TGA) was used to investigate experimentally the thermal decomposition behavior of PVA/MMT nanocomposites crosslinked at a dose of 20 kGy of electron beam irradiation. Figure 6 shows the initial TGA thermograms relating the percentage weight remaining (reactant mass) at different decomposition temperatures. In addition, the percentage weight loss at different heating temperatures is shown in Table II. It can be seen that the thermal decomposition of either PVA bulk polymer or PVA/MMT clay nanocomposites passes through three stages upon heating from room temperature to 500°C. Within the first stage up to 225°C, there is nearly no difference in thermal stability between PVA bulk polymer and PVA/MMT clay nanocomposites. However, it can be observed that the major decomposition occurs within the temperature range of 225–300°C, in which PVA polymer displayed the lowest thermal stability. Within this range, the thermal stability of PVA/MMT nanocomposites was found to decrease with increasing the MMT content displaying an increase in percentage weight loss. In the third region (300–500°C), the PVA nanocomposites loaded with 1 and 3% of MMT clay still possess higher thermal stability than neat PVA polymer. This trend can also be determined from the mid-point of the decomposition (the temperature at which 50% of the sample weight is lost) as shown in Table II. These findings are in accordance with the results obtained by Strawhecker and Manias

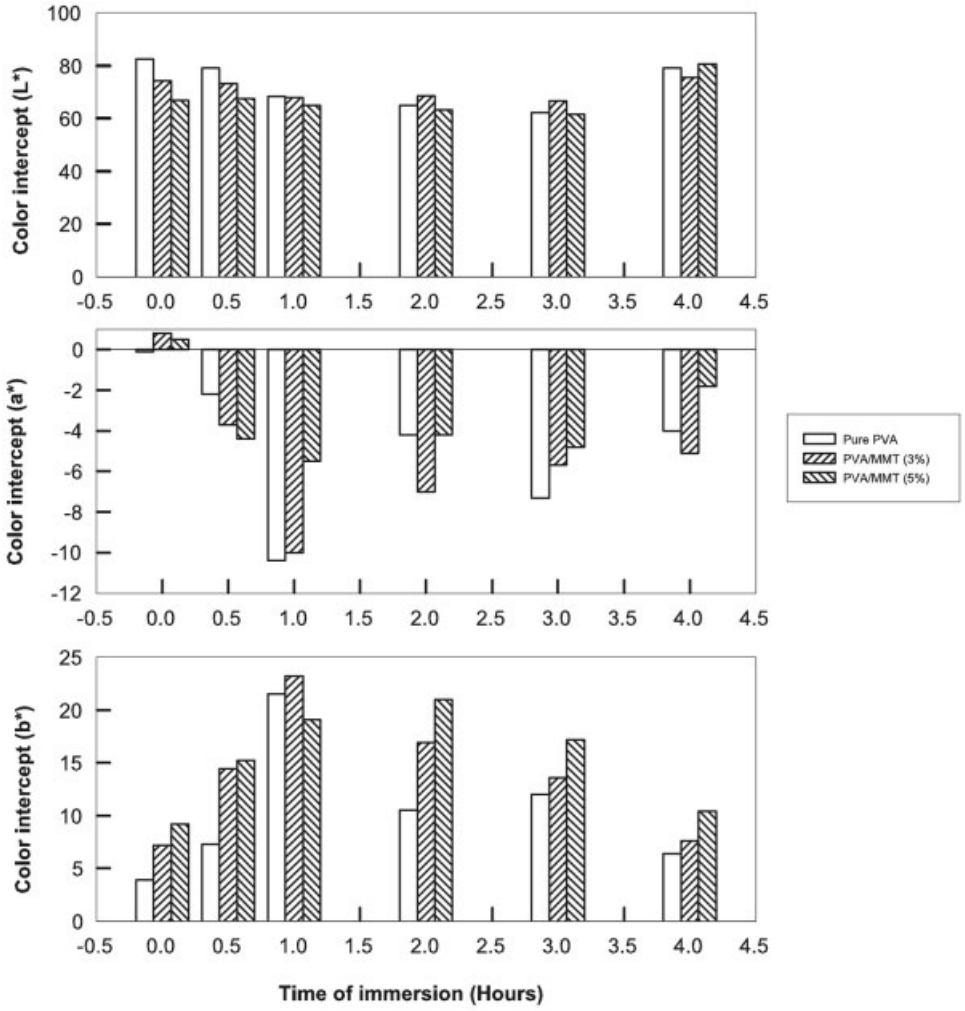

Figure 4 Color intercepts of pure PVA polymer and different PVA/MMT nanocomposites films formed at a dose of 20 kGy of electron beam irradiation before and after immersion in copper salt solutions for various lengths of times.

in a study on the thermal decomposition of non-crosslinked PVA/MMT nanocomposites prepared by solution-intercalation film casting method.[13]

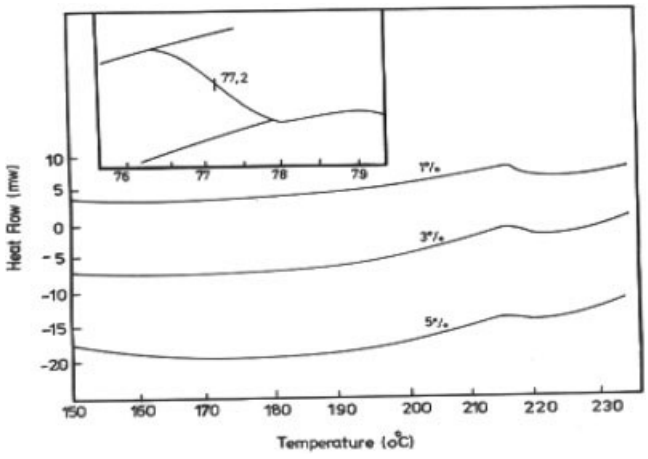

Figure 5 DSC scans of pure PVA (upper figure) and PVA/MMT nanocomposites with different contents of MMT clay formed at a dose of 20 kGy of electron beam irradiation.

The rate of reaction (dw/dt) was also plotted against the temperature over the range of 100–350°C as shown in Figure 7. The T_{max} (the temperature at which maximum value of the rate of reaction occurs) showed that the increase of MMT ratio from 1 to 4 wt % was accompanied with improvement in thermal decomposition. However, the increase of MMT content to 5% leads to a decrease in the T_{max} as shown in Table III.

As seen from the TGA thermograms and the rate of reaction curves (dw/dt), it is difficult to determine exactly the thermal decomposition of these systems. The thermal stability was further confirmed by determining the kinetic parameters of the thermal decomposition reactions. A method based on the rate of reaction proposed by Anderson and Freeman[20] was utilized, in which the quantities $\Delta\log(dw/dt)$ and $\Delta\log\hat{w}$ corresponding to a constant small difference of $\Delta(1/T)$ over the entire course of the initial TGA curve were first determined. The Anderson–Freeman equation, which relates these quantities, is given below:

$$\Delta\log(dw/dt)) = n\Delta\log\hat{w} - (E^*/2.303R)\Delta(1/T)$$

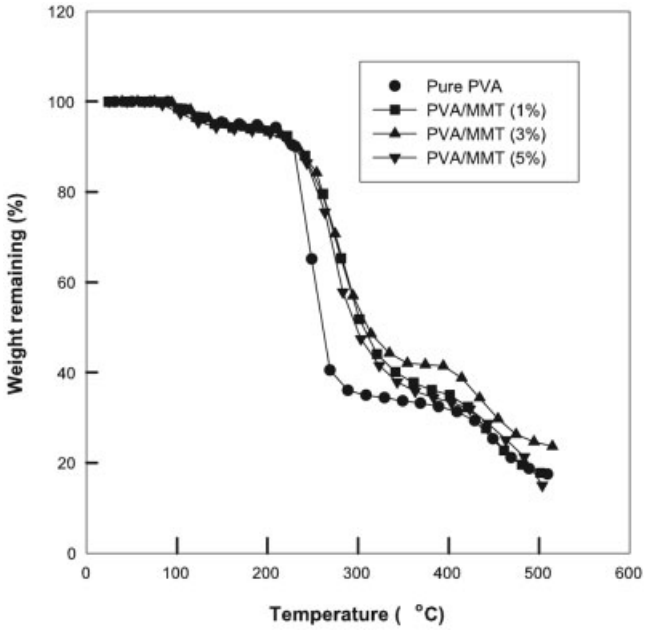

Figure 6 Initial TGA thermograms for pure PVA, PVA/MMT (1%), PVA/MMT (3%), and PVA/MMT (5%) nanocomposites films formed at a dose of 20 kGy of electron beam irradiation.

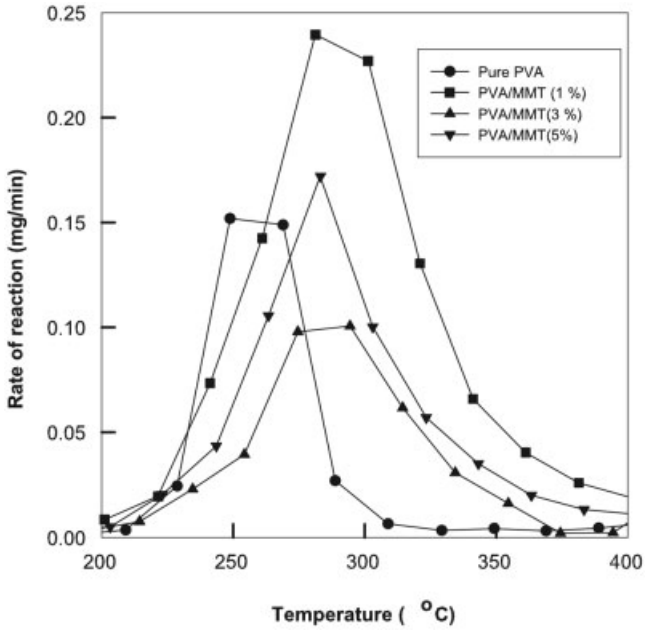

Figure 7 Rate of reaction (dw/dt) against temperature for pure PVA, PVA/MMT (1%), PVA/MMT (3%), and PVA/MMT (5%) nanocomposites formed at a dose of 20 kGy of electron beam irradiation.

where dw/dt is the rate of thermal decomposition reaction (mg min^{-1}), $\hat{w}$ is the reactant mass (mg), R is the gas constant (J mol^{-1} K^{-1}), E^* is the activation energy (J mol^{-1}), and n is the order of reaction. When $\Delta\log(dw/dt)$ is plotted against $\Delta\log \hat{w}$, it gives a straight line of slope 'n' and the intercept gives the activation energy E^*. The procedure and application of this method have been described elsewhere.[21,22] Figures 7 and 8 show the plots of Anderson–Freeman method, from which the activation energy can be calculated.

Based on the kinetic study, few conclusions may be made: (1) when $\Delta\log(dw/dt)$ was plotted against $\Delta\log \hat{w}$ for PVA/MMT with 1 and 5 wt % of MMT over the low range of temperatures, the data points did not fall on a straight line. Therefore, based on the Anderson–Freeman equation the thermal decomposition of these materials does not depend on the residual mass but on temperature and follows a zero order reaction. In this case, $\log(dw/dt)$ is plotted against $1/T$ and the slope is equal to $E^*/2.303R$, from which the activation energy can be calculated as shown in Figure 8. However, when $\Delta\log(dw/dt)$ was plotted against $\Delta\log \hat{w}$ for the same samples within the high temperature, the data points fall on a straight line as shown in Figure 9. An opposite trend was observed in the case of pure PVA, in which the thermal decomposition reaction shows a zero order reaction within the high range of temperature and first order within the low range of temperatures. (2) Calculated activation energy for the thermal decomposition reaction of pure PVA, PVA/MMT (1%), and PVA/MMT (5%) during the high range of temperatures (300–500°C) was found to be 107, 262, and 606 kJ mol^{-1}, respectively. (3) In conclusion, the intercalation of PVA with MMT clay improved greatly the thermal stability of PVA.

TABLE II
Weight Loss (%) at Different Heating Temperatures for the Thermal Decomposition of Pure PVA and PVA/MMT Nanocomposite Gels with Different MMT Contents

PVA nanocomposites	Weight loss (%)						
	100°C	200°C	300°C	350°C	400°C	450°C	500°C
Pure PVA	1.8	5.7	65.0	66.3	68.7	74.7	82.5
PVA/MMT (1%)	1.4	6.9	49.8	57.4	60.3	69.2	76.1
PVA/MMT (3%)	3.1	7.3	54.3	62.6	67.0	72.2	86.2
PVA/MMT (4%)	1.3	6.9	60.8	69.3	73.1	78.0	84.4
PVA/MMT (5%)	1.0	6.6	66.0	70.9	73.5	78.2	84.0

TABLE III
Thermal Properties of PVA/MMT Nanocomposites with Different MMT Contents

Temperature (°C)	MMT content (wt %)				
	Neat PVA	1	3	4	5
$T_{d1/2}$	259	310	298	290	275
T_{max}	250	290	290	290	270

Structure morphology of PVA/MMT nanocomposites

The strength of interfacial interactions between the polymer matrix and layered clay were investigated by examining the fracture surfaces by using scanning electron microscopy (SEM) as shown in Figure 10. The SEM micrograph of pure PVA is characterized with smooth surface. On the other hand, the SEM micrographs of PVA/MMT nanocomposites showed a different morphology, in which the surface is affected by the intercalation with the MMT clay. It is characterized by the hybrid structure, which appeared as separated parallel layers of ~4 μm apart particularly in the case of the nanocomposites with 4% MMT. This layered structure was not clear in the case of the nanocomposites with the low MMT of 1%, in which the fracture surface starts to align in layers indicating the presence of intercalation in accordance with XRD analysis.

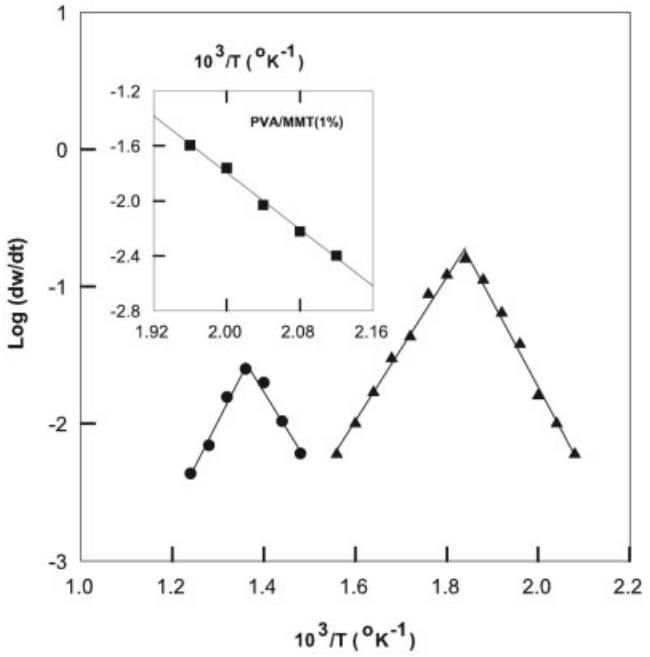

Figure 8 Temperature dependency of the logarithm of the rate of reaction of the thermal decomposition for (●) pure PVA, (■) PVA/MMT (1%), and (▲) PVA/MMT (5%) nanocomposites gels formed at a dose of 20 kGy of electron beam irradiation.

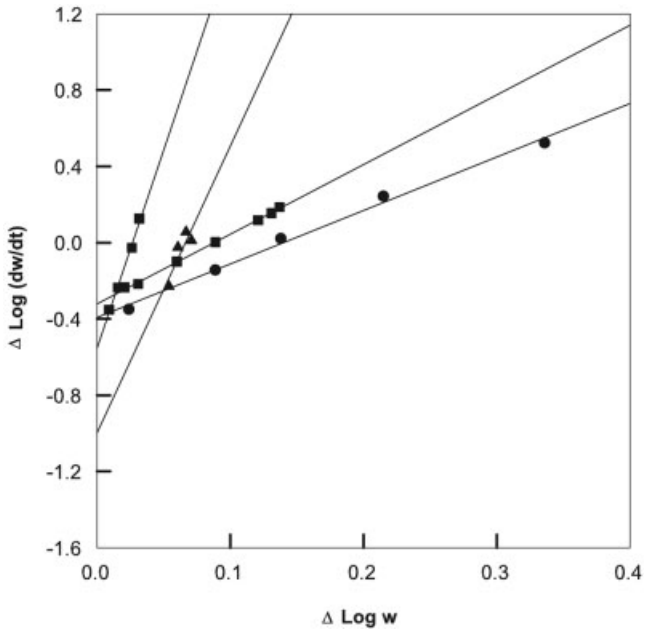

Figure 9 Anderson plots for the thermal decomposition of pure PVA nanocomposites gels hybrids with different contents of MMT clay formed at a dose of 20 kGy of electron beam irradiation. (●) PVA, (■) PVA/MMT (1%), and (▲) PVA/MMT (5%).

Mechanical properties of PVA/MMT nanocomposites

The main advantage of exfoliated polymer/clay nanocomposites containing microsized aluminosilicate sheets that dispersed in a polymer matrix associated with improved mechanical properties.[9] In general, the stress–strain curves of pure PVA polymer or PVA/MMT nanocomposites showed no yielding characteristics. Figure 11 shows the relationship between the MMT content and tensile strength and elongation at break of PVA/MMT nanocomposites. The tensile strength of PVA/MMT nanocomposites increases with increasing the MMT content up to 3 wt %. In this regard, the tensile strength was increased from 17.5 MPa for pure PVA to 50 MPa for PVA/MMT nanocomposites (3 wt %), i.e., the tensile strength was increased by 185.7%. This result indicates that PVA was strengthened by the introduction of exfoliated MMT, due to strong interfacial interaction between MMT and PVA matrix in accordance with the work reported in the case of polyimide/MMT.[23] Also, in accordance with that reported by Chen et al. regarding the role of clay as a reinforcing agent in PVA matrix for maleic anhydride modified polypropylene (MAPP)/organoclay nanocomposites.[24] They referred the improvement in mechanical properties due to the interfacial bonding between layered silicates and PVA, which leads to exfoliation of clay among the polymer matrix. On the other hand, the elongation at breaks of

the nanocomposites increases with increasing of the MMT content up to 4 wt %. In this regard, it was increased from 35% for pure PVA to 86% for PVA/MMT (4 wt %), i.e., elongation of this nanocomposite was increased by 145.7%.

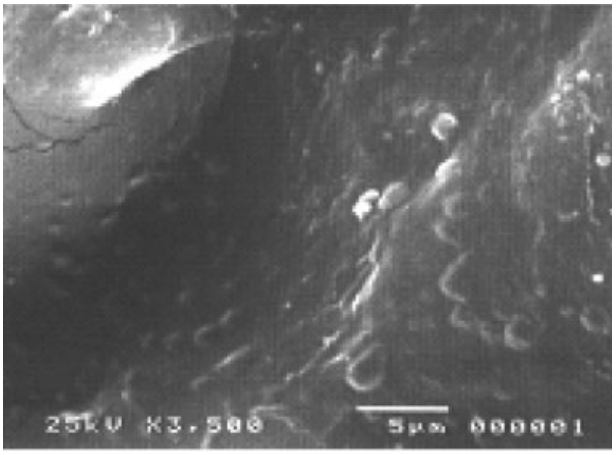

(a)

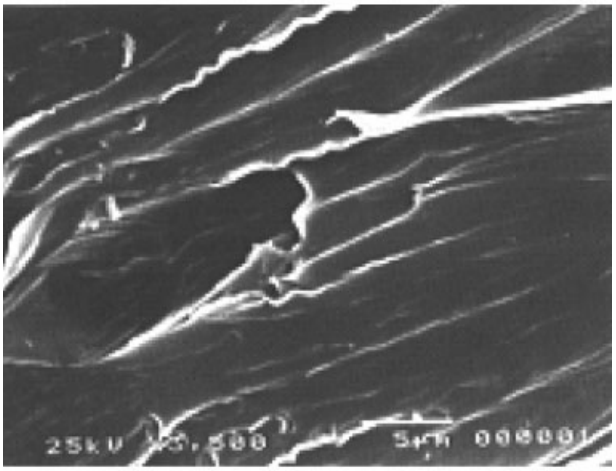

(b)

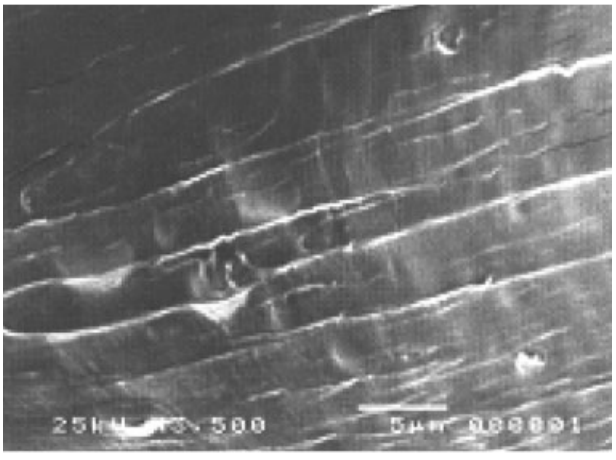

(c)

Figure 10 SEM micrographs of (a) pure PVA, (b) PVA/MMT (1 wt %), and (c) PVA/MMT (4 wt %).

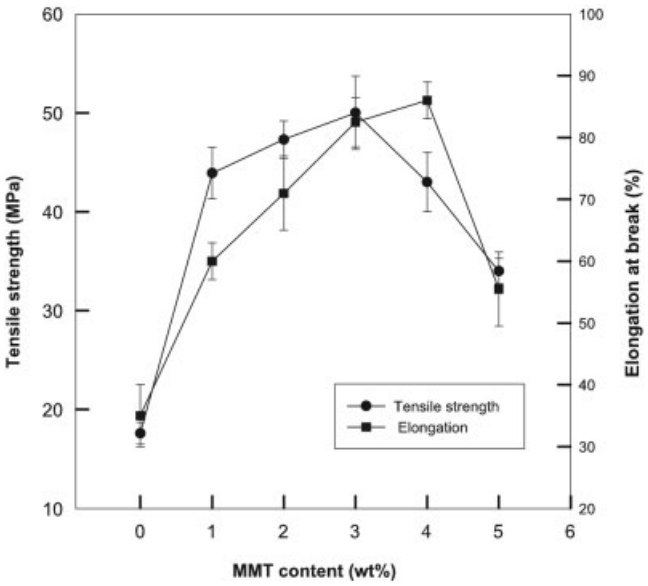

Figure 11 Tensile strength and elongation at break (%) as a function of MMT content for PVA/MMT clay nanocomposites electron beam crosslinked at a dose of 20 kGy.

CONCLUSIONS

This work focuses on the possible formation of nanocomposites gels based on hybrid films of PVA and MMT clay at various contents (1–5 wt %) under the effect of electron beam irradiation. The effect of intercalation on the thermal properties in terms of glass transition, melting transition, metal uptake, and mechanical properties was studied. Homogeneous PVA/MMT nanocomposites gels were obtained when the MMT content was 1–3 wt %. The introduction of MMT leads to significant improvement in thermal stability and mechanical properties such as tensile strength and elongation at break. The gels of PVA/MMT nanocomposites exhibit a high resistance to water absorption. The intercalation with MMT clay suppressed the glass transition temperature of PVA and did not affect the melting transition.

References

1. Chigwada, G.; Wilkie, C. A. Polym Degrad Stab 2003, 80, 551.
2. Alexandre, A.; Dubois, P. Mater Sci Eng 2000, 28, 1.
3. Liang, Z.; Yin, J.; Wu, J.; Qiu, Z.; He, F. Eur Polym J 2004, 40, 307.
4. Ray, S.; Okamoto, M. Prog Polym Sci 2003, 28, 1539.
5. Ebdon, J. R.; Hunt, B.; Joseph, P. J. Polym Degrad Stab 2004, 83, 181.
6. Uhl, F. M.; Wilkie, C. A. Polym Degrad Stab 2002, 76, 111.
7. Xu, Y.; Brittain, W. J.; Xue, C.; Eby, R. K. Polymer 2004, 45, 3735.
8. Wang, J.; Du, J.; Zhu, J.; Wilkie, C. A. Polym Degrad Stab 2002, 77, 249.
9. Davis, R. D.; Gilman, J. W.; Vaderhart, D. W. Polym Degrad Stab 2003, 79, 111.
10. Pramoda, K. P.; Liu, T.; Liu, Z.; He, C.; Sue, H. J. Polym Degrad Stab 2003, 81, 47.

11. Vaia, R. A.; Vasudevan, S.; Krawiec, W.; Scanlon, L. G.; Giannelis, E. P. J Polym Sci Part B: Polym Phys 1997, 35, 59.
12. Carrado, K. A.; Thiyagarujan, P.; Elder, D. L. Clays Clay Miner 1996, 44, 506.
13. Strawhecker, K. E.; Manias, E. Chem Mater 2000, 12, 2943.
14. Guangyao, S. S.; Stephen, A. B. Environ Sci Technol 1996, 30, 1553.
15. Bozena, P.; Stawomir, S.; Beata, J.; Lars-Ake, L.; Jerzy, P. Appl Clay Sci 2004, 25, 221.
16. Doppers, L. M.; Breen, C.; Sammon, C. Vib Spectrosc 2004, 35, 27.
17. Yu, Y. H.; Lin, C. Y.; Yeh, J. M.; Lin, W. H. Polymer 2003, 44, 3553.
18. Anastasiadis, S. H.; Karatasos, K.; Giannelis, E. P.; Manias, E. Phys Rev Lett 2000, 84, 915.
19. Bandyopadhyay, S.; Giannelis, E. P. Polym Mater Sci Eng 2000, 82, 208.
20. Anderson, D. A.; Freeman, E. S. J Polym Sci 1961, 54, 253.
21. El-Salmawi, K.; Abu Zeid, M. M.; El-Naggar, A. M.; Mamdouh, M. J Appl Polym Sci 1999, 72, 509.
22. Nizam El-Din, H. M.; El-Naggar, A. M.; Ali, F. I. Polym Int 2003, 52, 225.
23. Biswas, M.; Ray, S. S. Adv Polym Sci 2002, 155, 167.
24. Chen, L.; Wong, S. C.; Pisharath, S. J Appl Polym Sci 2003, 88, 3298.